



Synthesis of mannoheptose derivatives and their evaluation as inhibitors of the lectin LecB from the opportunistic pathogen *Pseudomonas aeruginosa*

Anna Hofmann^{a,†,‡}, Roman Sommer^{a,b,c,‡}, Dirk Hauck^{a,b,c}, Julia Stifel^a, Inigo Göttker-Schnetmann^a, Alexander Titz^{a,b,c,*}

^a Department of Chemistry and Graduate School Chemical Biology, University of Konstanz, D-78457 Konstanz, Germany

^b Chemical Biology of Carbohydrates, Helmholtz Institute for Pharmaceutical Research Saarland (HIPS), D-66123 Saarbrücken, Germany

^c Deutsches Zentrum für Infektionsforschung (DZIF), Standort Hannover-Braunschweig, Germany

ARTICLE INFO

Article history:

Received 23 December 2014

Received in revised form

2 April 2015

Accepted 3 April 2015

Available online 5 May 2015

Keywords:

Lectin

Pseudomonas aeruginosa

Inhibitor

ABSTRACT

Biofilm formation and chronic infections with *Pseudomonas aeruginosa* depend on lectins produced by the bacterium. The bacterial C-type lectin LecB binds to the two monosaccharides L-fucose and D-mannose and conjugates thereof. Previously, D-mannose derivatives with amide and sulfonamide substituents at C6 were reported as potent inhibitors of the bacterial lectin LecB and LecB-mediated bacterial surface adhesion. Because D-mannose establishes a hydrogen bond via its 6-OH group with Ser23 of LecB in the crystal structure and may be beneficial for binding affinity, we extended D-mannose and synthesized mannoheptoses bearing the free 6-OH group as well as amido and sulfonamido-substituents at C7. Two series of diastereomeric mannoheptoses were synthesized and the stereochemistry was determined by X-ray crystallography. The potency of the mannoheptoses as LecB inhibitors was assessed in a competitive binding assay. The data reveal a diastereoselectivity of LecB for (6S)-mannoheptose derivatives with increased activity over methyl α -D-mannoside.

© 2015 Elsevier Ltd. All rights reserved.

1. Introduction

The Gram-negative bacterium *Pseudomonas aeruginosa* is an opportunistic human pathogen that is responsible for an extensive part of nosocomial infections.^{1,2} In immuno-compromised patients or individuals with the genetic disease cystic fibrosis, the bacterium can establish chronic infections, which can lead to organ failure and death of the patient.³ In addition to its high level of multidrug resistance *P. aeruginosa* can live in biofilms, which provide an additional protection against hostile environment such as the immune defense or antibiotic treatment.^{4,5} Bacterial biofilms are multicellular communities in which bacterial cells are embedded in a self-produced matrix, consisting of exopolysaccharides, extracellular DNA, lipids and proteins.⁶

* Corresponding author.

E-mail address: alexander.titz@helmholtz-hzi.de (A. Titz).

† Current address: Institute of Pharmacy and Food Chemistry, University of Würzburg, D-97074 Würzburg, Germany.

‡ Both authors contributed equally.

For *P. aeruginosa* the two bacterial lectins LecA and LecB (formerly named PA-IL and PA-IIL, respectively) are involved in biofilm formation and knock-out strains show reduced biofilm mass.^{7,8}

LecB was initially isolated by Gilboa-Garber et al. and a glycan-binding specificity for L-fucose and D-mannose was found.^{9,10} The structure of LecB was solved by X-ray crystallography and revealed a non-covalent tetrameric assembly with the carbohydrate binding sites oriented towards the vertices of a tetrahedron.^{11,12} The carbohydrate ligands L-fucose or D-mannose are bound via all three secondary hydroxy groups in the respective ligand to the two calcium ions in the carbohydrate recognition domain of LecB. Methyl α -L-fucoside shows an unusual high affinity for LecB ($K_d=430$ nM), whereas mannoside **1** (Fig. 1) is a 150-fold weaker ligand for the lectin ($K_d=71$ μ M).¹³ The fucose-containing trisaccharide Lewis^a was identified as its strongest monovalent ligand ($K_d=210$ nM).¹⁴ Consequently, a number of fucose derivatives have been developed and evaluated for LecB inhibition, often on multivalent display as a technique to improve binding affinities.^{15–18} Reymond and co-workers developed a fucosylated multivalent glycopeptide

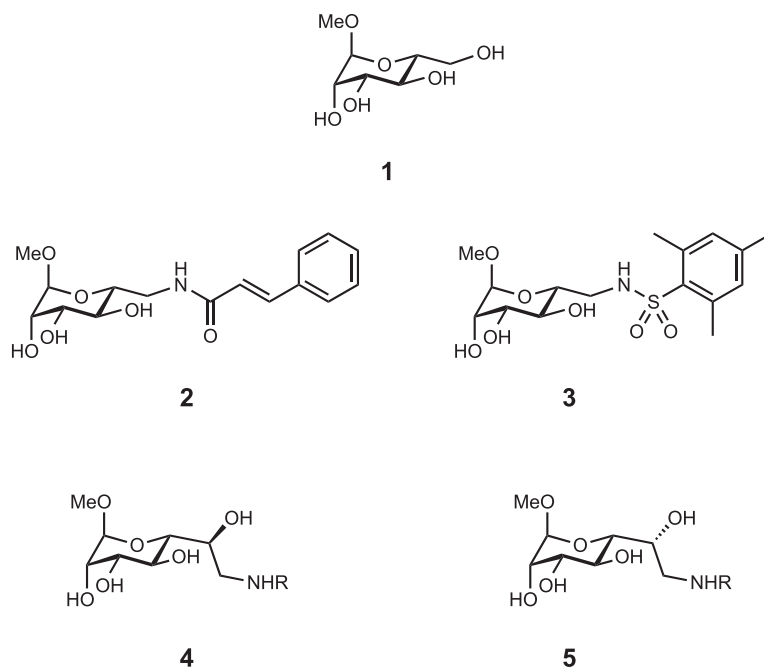


Fig. 1. The LecB ligand methyl α -D-mannoside (**1**) forms a hydrogen bond through its 6-hydroxy group with Ser23. Mannose derivatives **2** and **3** are high affinity inhibitors of LecB, although unable to establish a hydrogen bond with Ser23. Mannoheptose derivatives **4** and **5** were designed to allow possible hydrogen bond formation of their 6-hydroxy group with Ser23 and attachment of additional pharmacophores (R).

dendrimer, which inhibits the formation of *P. aeruginosa* biofilms in a LecB-dependent manner.¹⁹ Recently, Vidal and co-workers reported fucosylated tetravalent glycoclusters on a calixarene scaffold as high-affinity ligands for LecB, which reduced *P. aeruginosa*-induced lung injury as well as bacterial load in lung and spleen tissue.²⁰ All fucose-based inhibitors of LecB bear unmodified terminal α -L-fucosyl residues, an epitope, which is recognized by numerous lectins of the host immune system, e.g. the selectins, DC-SIGN, MBL and others. In order to potentially increase target specificity and reduce interference with host lectins, we recently reported high affinity mannose-based LecB inhibitors **2** and **3** with a camouflaged mannosyl residue through capping at C6.²¹

In contrast to its low affinity for this lectin, D-mannose forms an additional hydrogen bond in the crystal structure of its O6 with LecB at residue Ser23.¹² Interestingly, this hydrogen bond does not contribute significantly to the overall binding affinity at ambient conditions.²² This observation could result from a high degree of flexibility of **1** in the unbound state, and thus increased entropy costs upon binding, a concept well established for the C-type lectin E-selectin and its carbohydrate ligand sialyl Lewis^x.^{23–27} Extension of mannose-derived ligand **1** with additional pharmacophores at C6 allows the targeting of adjacent protein surface and potent inhibitors, e.g. **2** and **3** (Fig. 1), were obtained.²¹ Although these compounds are LecB inhibitors with more than 20-fold improved affinity, the hydrogen bond with Ser23 cannot be established due the lack of O6. Additionally exploiting the interaction of Man-O6 by increasing its attractive potential could lead to superior inhibitors. For example, rigidification of Man-O6 in its crystal-observed bioactive orientation through assistance of closely protein bound adjacent pharmacophores is a promising approach. To analyze the effect of a hydrogen bonding interaction of O6 in addition to the presence of further pharmacophores targeting the adjacent protein surface on LecB-binding, we designed mannoheptosides **4** and **5** (Fig. 1). The synthesis of both diastereomers should allow the assessment of the influence of the stereochemistry at C6 on the binding affinity to LecB. Further attachment of pharmacophores on

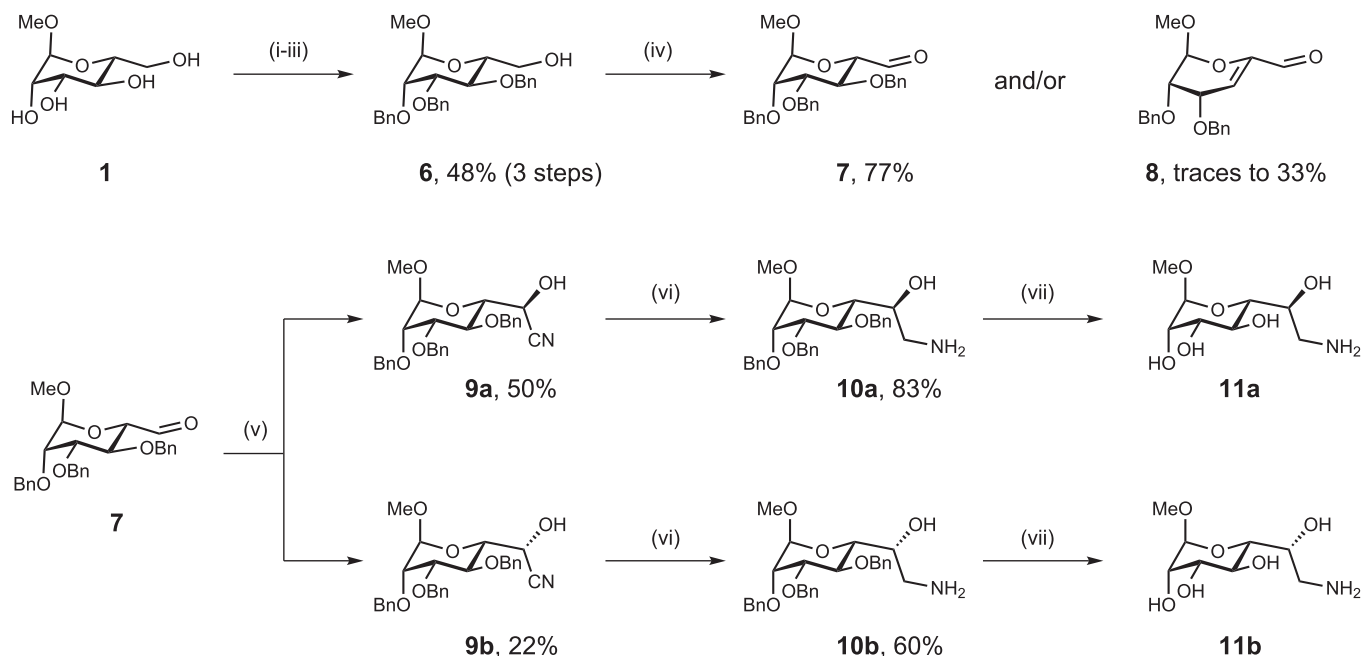
the nitrogen atom at C7 can then be performed to target the adjacent protein surface.

Here, we report the chemical synthesis of two sets of diastereomeric mannoheptoses and the optimization of the reaction sequence Swern oxidation, cyanohydrin formation and subsequent reduction to the amine. Finally, the compounds obtained in the two diastereomeric series were evaluated in a competitive binding assay for their binding affinity to LecB.

2. Results and discussion

The synthesis of the diastereomeric mannoheptosides **4** and **5** was initiated by transforming commercial methyl α -D-mannoside (**1**) according to published procedures into the selectively protected mannoside **6**²⁸ with a free 6-hydroxy group allowing further manipulation (Scheme 1). Therefore, **1** was trityl-protected at O-6, subsequently benzylated at the 2-, 3- and 4-hydroxy groups and detritylated using iron(III) chloride²⁹ without purification of the intermediates on a 35 g scale in 48% yield over three steps. Oxidation of the primary hydroxy group in **6** to the aldehyde **7** was performed under Swern conditions.

In a first Swern oxidation, the reaction yielded the desired product **7** in 34% and α,β -unsaturated elimination product **8** in 33% after workup without neutralization of the triethylamine (Table 1, entry 1). Mackie and Perlin³⁰ reported similar base-induced elimination products after Swern oxidation for acylated pyranosides. The acetates reported by Mackie and Perlin are however much better leaving groups than benzylic alcoholate as it is present as leaving group at the 4-position in precursor **6**. In a series of reactions to avoid elimination, the water bath temperature for solvent removal was reduced, excess of triethylamine was reduced and either volatiles were removed directly or after aqueous workup (entry 2–4). Aldehyde **7** was finally obtained in 77% yield after initial neutralization of the reaction and subsequent purification (entry 5).



Scheme 1. Synthesis of methyl α -D-manno-7-amino-7-deoxy-heptapyranosides **11a** and **11b**: (i) Ph_3CCl , pyr, rt, (ii) NaH, PhCH_2Br , DMF, 0°C –rt, (iii) $\text{FeCl}_3 \cdot 6\text{H}_2\text{O}$, CH_2Cl_2 , rt, (iv) $(\text{COCl})_2$, DMSO, NEt_3 , CH_2Cl_2 , -75°C –rt, (v) KCN, MeOH, NH_4Cl (aq), 0°C –rt, (vi) LiAlH_4 , THF, 0°C –rt, (vii) Pd–C, H_2 (1 bar), H_2O , THF, TFA, rt. **11a** and **11b** were obtained as crude products and used without further purification.

Table 1
Optimization of the Swern oxidation (**6** \rightarrow **7**) workup procedure to prevent formation of elimination product **8**

Entry	NEt_3 [eq.]	Workup procedure	7 [%] ^a	8 [%] ^a
1	5	Quenching (H_2O), extraction (CH_2Cl_2), solvent removal in vacuo (40°C)	34	33
2	5	Direct solvent removal in vacuo (30°C)	43	—
3	2.5	Quenching (H_2O), extraction (CH_2Cl_2), solvent removal in vacuo (30°C)	68	—
4	2.5	Direct solvent removal in vacuo (30°C)	70	Traces (TLC)
5	2.5	Quenching (satd. NH_4Cl aq), wash (H_2O), extraction (CH_2Cl_2), solvent removal in vacuo (30°C)	77	Traces (TLC)

^a Isolated yields.

The mannoheptose motif was then established by cyanohydrin formation with aldehyde **7** and potassium cyanide. Because of its basicity and potential to induce elimination in **7**, we tested various aqueous buffered conditions for the addition reaction (Table 2). The transformation (**7** \rightarrow **9**) was performed using common buffers with pH values ranging from 4.5 to 8.0 and the product was obtained as a separable diastereomeric mixture **9a** and **9b**, with slightly varying diastereoselectivity from 1.8:1 to 2.3:1. The ammonium chloride buffered system was used on preparative scale and isolated **9a** and isolated **9b** could be obtained in 50% and 22% yield, respectively. To determine the absolute configuration at C6 of diastereomers **9a** and **9b**, we performed ^1H NMR experiments with J-coupling analysis as well as J-HMBC NMR experiments. In non-polar solvents such as deuterated chloroform, compounds **9a** and **9b** can potentially establish an intramolecular hydrogen bond between the 6-hydroxy

group and the oxygen atom at position 4 (Fig. 2A). Assuming such a conformation, a gauche orientation between H5 and H6 for **9a** and a trans orientation for both nuclei in **9b** would lead to small and large ^3J -coupling constants respectively, following the Karplus equation. However, only small coupling constants for both diastereomers were observed: $^3\text{J}_{5,6}=1.1$ Hz for **9a**, $^3\text{J}_{5,6}=4.0$ Hz for **9b**. Varying the temperature during NMR analysis to observe the potential 6-membered ring at reduced temperature only gave line broadening and signal overlap (see Supplementary data). Similar to ^1H , ^1H coupling, the Karplus equation also describes ^3J -coupling constants between ^1H and ^{13}C nuclei. To avoid the problem of signal overlap in 1D spectra, we therefore analyzed **9a** and **9b** in a two-dimensional J-HMBC NMR³¹ experiment to determine the coupling constants between H5 and the nitrile carbon C7 of the two isomers. Again, comparable coupling constants were observed:

Table 2
Optimization of the cyanohydrin formation (**7** \rightarrow **9**) to prevent KCN-induced formation of elimination product **8** and to analyze buffer influence on diastereoselectivity^a

Entry	Buffer system	Conc. [M]	pH	8 [%]	d.r. 9a:9b (^1H NMR)	Isolated yield [%]
1	Tris–HCl	1	7.0	—	1.8:1	—
2	$\text{K}_2\text{HPO}_4/\text{KH}_2\text{PO}_4$	1	7.4	—	2:1	—
3	NaHCO_3	1	8.0	—	2:1	—
4	NH_4Cl	6	4.5	Traces	2.3:1	9a 50%, 9b 22%

^a Diastereomeric ratios were determined on crude products by ^1H NMR.

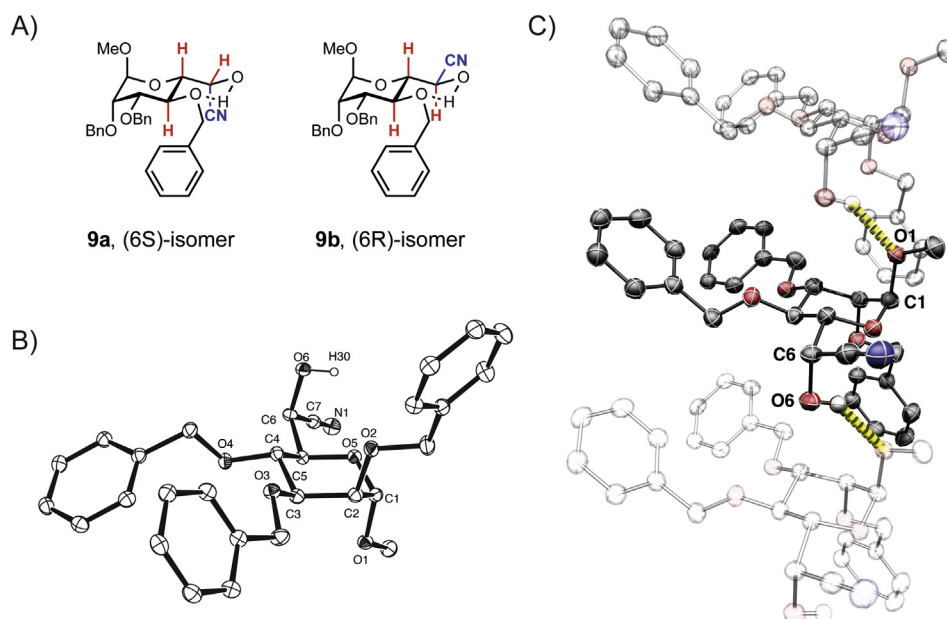


Fig. 2. Structure determination of diastereomeric cyanohydrins: A) hypothetical intramolecular hydrogen bonding leads to a six-membered ring. Analysis of ^1H , ^1H -homonuclear and ^1H , ^{13}C -heteronuclear ^3J NMR coupling constants of protons H-4, -5 and -6 and the nitrile carbon atom could explain the stereochemistry at C6 due to *trans*- and *gauche* orientations in a potential 6-membered ring in CDCl_3 . B) The crystal structure of **9a** shows the (6*S*)-configuration of the cyanohydrin. C) In the packing of the crystal structure, the 6-hydroxy group forms an intermolecular hydrogen bond and does not form a possible 6-membered ring structure as hypothesized (carbon atoms are shown black, oxygen red, nitrogen blue). (For interpretation of the references to colour in this figure legend, the reader is referred to the web version of this article.)

$^3\text{J}_{\text{H5,C7}}=9.9$ Hz for **9a**, $^3\text{J}_{\text{H5,C7}}=8.8$ Hz for **9b** (Table S1). Due to the absence of signal overlap in the 2D spectrum, temperature variation and determination of $^3\text{J}_{\text{H5,C7}}$ coupling constant values over a temperature range from 215–292 K could be performed for **9a** and **9b**. However, no clear trend towards larger coupling constants in one of the two diastereomers could be detected to unambiguously assign its stereochemistry. Finally, **9a** could be crystallized by slow evaporation in a methylene chloride–pentane mixture. The crystal structure determines the (6*S*)-configuration in **9a** (Fig. 2B, Table S2) and consequently, **9b** is the (6*R*)-diastereomer. Interestingly, in the crystalline state **9a** does not form the anticipated intramolecular hydrogen bond for the solution experiments, but its 6-OH forms an intermolecular hydrogen bond with O1 of the neighboring molecule in the crystal lattice (Fig. 2C). The dihedral angle O5–C5–C6–O6 of cyanohydrin **9a** has a value of -63.18° in the crystal structure (Fig. 2B), whereas in case of the anticipated intramolecular hydrogen bond this dihedral angle corresponds to 180° in both diastereomers (Fig. 2A).

After establishing the stereochemical configuration of the cyanohydrins, **9a** and **9b** were reduced to the primary amines **10a** and **10b**, respectively (Scheme 1). Nickel-catalyzed borane reduction in *iso*-propanol as reported by Lu et al.³² for structurally more simple

cyanohydrins to the corresponding amino alcohol was unsuccessful for the diastereomeric mixture **9ab** (Table 3, entry 1–3) and product could not be detected. Attempts to reduce **9ab** using sodium borohydride with or without aluminum chloride only gave the primary alcohol **6**, presumably by rapid elimination of the nitrile and subsequent reduction of the aldehyde **7** (entry 4, 5). The use of lithium aluminum hydride as reported by Dziewiszek and Zamojski³³ for related mannoheptoses was finally successful to transform **9a** into **10a** in 83% yield and **9b** into **10b** in 60% yield, respectively (entry 6, 7). Palladium-catalyzed hydrogenolytic cleavage of the benzyl groups required the presence of 0.35% trifluoroacetic acid in the solvent system tetrahydrofuran–water³⁴ for successful transformation of benzylated **10a** into amino heptose **11a** and diastereomer **10b** into **11b**. Hydrogenation attempts using methanol or dioxane as solvents and acetic acid as activator were unsuccessful. Furthermore, direct hydrogenation of benzylated cyanohydrin **9a** to the fully deprotected amine **11a** was successful on analytical scale using the same solvent system TFA/THF/ H_2O . However, it was accompanied by a significant fraction of side product with m/z 430 found in LC-MS, which could be a product of the reaction of **11a** with the intermediate imine, subsequent elimination of ammonia and hydrogenolysis of the N-alkylated imine

Table 3
Reaction conditions tested to reduce cyanohydrins **9a** and **9b** to amines **10a** and **10b**

Entry	Starting material	Reaction conditions	Product
1	9ab	BH_3^*THF (12 equiv), <i>iso</i> -PrOH, NiCl_2 (satd), 18 h, 0°C –rt.	—
2	9ab	BH_3^*THF (12 equiv), <i>iso</i> -PrOH, NiCl_2 (3 equiv), 6 h, 0°C –rt.	—
3	9ab	BH_3^*THF (16 equiv), <i>iso</i> -PrOH, NiCl_2 (3 equiv), 6 h, 0°C –rt.	—
4	9ab	NaBH_4 (4 equiv), THF, 6 h, rt.	6 ^a
5	9ab	NaBH_4 (4 equiv), THF, AlCl_3 (0.5 equiv), 6 h, rt.	6 ^a
6	9a	LiAlH_4 (4.5 equiv), THF, 15 min, 0°C –rt.	10a (83%) ^b
7	9b	LiAlH_4 (4.5 equiv), THF, 15 min, 0°C –rt.	10b (60%) ^b

^a Identity was determined by ^1H NMR analysis of the crude product.

^b Isolated yields.

leading to a secondary amine (MW=429 g/mol) as described by Rylander³⁵ for hydrogenolysis of nitriles and their common side products. Therefore, the two-step procedure using first a lithium aluminum hydride reduction of the nitriles and subsequent hydrogenolytic cleavage of the benzyl groups was performed.

Subsequently, crude amines **11a** and **11b** were transformed into amides **4a–c** and **5a–b** respectively (Scheme 2). The resulting amides of the (6*S*)-**4**- and the (6*R*)-**5**-series were then tested in the competitive binding assay for LecB inhibition (Table 4). We recently developed this binding assay, which relies on the competitive displacement of a fluorescein-fucose conjugate from the carbohydrate binding site of LecB and detection by fluorescence polarization.²¹ Interestingly, all tested compounds bound to LecB, although in the high micromolar range. Furthermore, the influence of the stereocenter at C6 on binding affinity towards LecB favors (6*S*)-mannoheptoses, with a selectivity of a factor of three. The data suggest either a reduced importance of the hydrogen bond established between 6-OH and Ser23 on binding affinity or a sterically unfavored interaction of the amide substituents introduced at C7. A combination of both effects could also lead to the observed negative influence on binding affinity, although large amide substituents introduced at the shorter C6 as in **2** generally led to increased binding affinities compared to **1**.²¹ Due to the better affinities in the (6*S*)-**4** series of amides, sulfonamides **4d** and **4e** were synthesized and evaluated in the binding assay for LecB. The introduction of sulfonamides at C7 of (6*S*)-mannoheptoses (**4d**, **4e**) lead to an additional two- to threefold improvement as compared to the (6*S*)-amides **4a–c**.

In summary, we have designed and synthesized a series of diastereomeric mannoheptoses with amide and sulfonamide substituents at C7 for the inhibition of the bacterial lectin LecB. Previously, *D*-mannose derivatives with amide and sulfonamide substituents at C6 (e.g., **2** and **3**) were reported as potent inhibitors of LecB. Because *D*-mannose establishes a hydrogen bond via its 6-OH group with Ser23 of LecB in the crystal structure,¹² we extended *D*-mannose and synthesized mannoheptoses bearing the free 6-OH group as well as amido and sulfonamido-substituents at C7 (**4a–e**, **5a–b**). Such compounds could allow the formation of a hydrogen

Table 4

Biochemical evaluation of heptosides **4a–e** and **5a–b** for LecB binding. IC₅₀ values are averages of at least three independent experiments, standard deviations are given. Data for **1**, **2** and **3** have been previously reported²¹

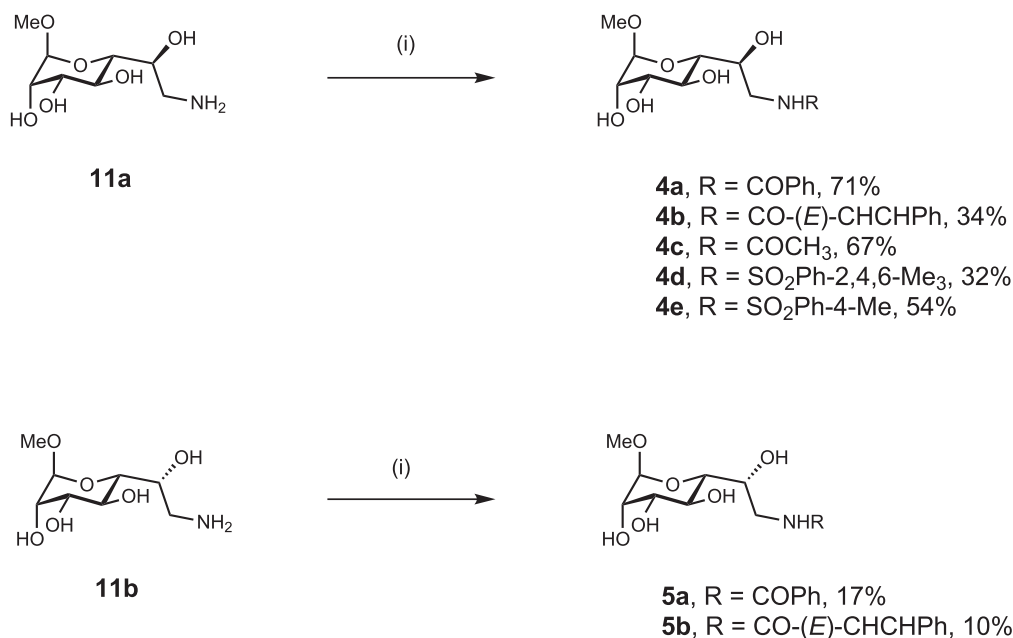
Entry	Compound	Configuration	IC ₅₀ [μM]
1	4a	6 <i>S</i>	180±25
2	4b	6 <i>S</i>	217±57
3	4c	6 <i>S</i>	198±111
4	4d	6 <i>S</i>	101±29
5	4e	6 <i>S</i>	82±23
6	5a	6 <i>R</i>	553±29
7	5b	6 <i>R</i>	546±60
8	1	—	158±53
9	2	—	37±5.0
10	3	—	3.4±0.4

bond with Ser23 and increase binding affinity due to additional pharmacophores attached at C7. The synthesis followed the route Swern oxidation at C6, cyanohydrin formation and subsequent reduction of the nitrile to the amine. All three reactions were optimized and the stereochemistry of one diastereomer (**9a**) was determined by X-ray crystallography. All final compounds were inhibitors of LecB in the micromolar range. Sulfonamides **4d** and **4e** displayed increased affinities compared to the lead structure **1**. The effect of the orientation of the hydroxy group at C6 on binding affinity was established with a selectivity of LecB for 6*S*-diastereomers, the magnitude of the effect indicated a reduced importance to the overall binding affinity in solution. The results obtained in this study will help to design more potent inhibitors of LecB as future therapeutics against chronic *P. aeruginosa* infections.

3. Experimental section

3.1. General experimental details

Commercially available chemicals were used without further purification. Dry solvents were acquired from VWR and Acros Organics. Thin layer chromatography (TLC) was performed using silica



Scheme 2. Synthesis of amide and sulfonamide derivatives **4** and **5**: (i) for **4a** and **5a**: benzoyl chloride, NEt₃, DMF; for **4b** and **5b**: cinnamic acid, EDC⁺HCl, NEt₃, DMF, 0 °C–rt.; for **4c**: acetic anhydride, NEt₃, DMF, 0 °C–rt.; for **4d** and **4e**: sulfonyl chloride, NEt₃, DMF, 0 °C–rt.; Isolated yields over two steps from **10a** and **10b**, respectively.

gel 60 aluminum plates containing fluorescent indicator from Merck and detected either with UV light at 254 nm or by charring in molybdate solution (0.02 M solution of $(\text{NH}_4)_4\text{Ce}(\text{SO}_4)_4 \cdot 2\text{H}_2\text{O}$ and $(\text{NH}_4)_6\text{Mo}_7\text{O}_{24} \cdot 4\text{H}_2\text{O}$ in aqueous 10% H_2SO_4), in Ekkert's reagent (1.5% *p*-anisaldehyde, 1.5% concentrated H_2SO_4 and 15% glacial acetic acid in EtOH), or in ninhydrin (0.05 M in EtOH) with heating. Solvents for flash chromatography were distilled before use. Flash chromatography was carried out at Combiflash Rf200 from Teledyne Isco using silica gel 60 M (particle size 40–63 μm). High resolution mass spectra were obtained on ESI Bruker MicroTOF II. NMR spectra were recorded on Bruker Avance III 400, 500 or 600 at 400/500/600 MHz (^1H) and 101/125/151 MHz (^{13}C). Chemical shifts are given in parts per million and were calibrated on internal standards of deuterium labeled solvents. Multiplicities were specified as s (singlet), d (doublet), dd (doublet of a doublet), ddd (doublet of a doublet of a doublet), t (triplet), m (multiplet). NMR assignments of new compounds were confirmed by $^1\text{H}, ^1\text{H}$ COSY, $^1\text{H}, ^{13}\text{C}$ HSQC and $^1\text{H}, ^{13}\text{C}$ HMBC experiments. IR spectra of solid compounds were recorded on a Spectrum 100 FT-IR spectrometer from Perkin Elmer with ATR sampling accessory. Optical rotation was measured on JASCO P-2000 polarimeter. Purification of compounds **4b–4e** and **5a/5b** by reversed phase HPLC was performed on a Shimadzu HPLC with an Agilent C18 column (30* 100 mm, 10 μm) using $\text{H}_2\text{O}/\text{MeCN}$ as mobile phase (0–5 min 5% MeCN; 5–25 min 5–60% MeCN; 25–35 min 60% MeCN; 35–40 min 60–95% MeCN; 40–45 min 95% MeCN; 45–50 min 95–5% MeCN; flow: 4 mL/min).

3.2. Crystal structure analysis of **9a**

Complete crystallographic data for the structural analysis have been deposited with the Cambridge Crystallographic Data Centre, CCDC no. 1026815. Copies of this information may be obtained free of charge from the Director, Cambridge Crystallographic Data Centre, 12 Union Road, Cambridge, CB2 1EZ, UK. (fax: +44 1223 336033, e-mail: deposit@ccdc.cam.ac.uk or via: www.ccdc.cam.ac.uk).

X-ray diffraction analysis was performed at 100 K on a STOE IPDS II diffractometer equipped with a graphite-monochromated radiation source ($\lambda=0.71073 \text{ \AA}$) and an image plate detection system. Crystals of **9a** suitable for X-ray diffraction analysis were grown from methylene chloride/pentane (1/7) solutions by slow evaporation of the solvent. A 0.45x0.25x0.15 mm crystal fragment of a 1.2x0.25x0.15 mm needle was mounted on the top of a glass-fiber by means of silicon-grease and placed on the goniometer head. A total of 240 frames with a width of 1° each (180 frames at $\text{phi}=0^\circ$, and 60 frames at $\text{phi}=90^\circ$) with an exposure time of 2.5 min was then collected. The selection, integration and averaging procedure of the measured reflex intensities, the determination of the unit cell dimensions and a least-square fit of the 2θ values as well as data reduction, LP-correction and space group determination were performed using the X-Area software package delivered with the diffractometer.³⁶ A semiempirical absorption correction was performed. The structure was solved by direct methods (SHELXS-97³⁷), completed with difference fourier syntheses, and refined with full-matrix least-square cycles using SHELXL-97 by minimizing $\omega(F_o^2 - F_c^2)^2$ including an extinction correction. Weighted R factor (wR_2) and the goodness of fit GooF are based on F^2 . The hydrogen atom H30 attached to O6 was located in the electron density map and refined isotropically without constraints. All other hydrogen atoms were refined in a riding model. The absolute stereochemistry of the model was not reliably determined by the X-ray diffraction experiment due to the absence of heavy atoms (>Si). However, the synthetic procedure for compound **9a** starts from methyl α -D-mannoside (**1**) and therefore the absolute stereochemistry is assumed as given in the model. Graphical output (Ortep plots) were created using Diamond Crystal or Molecular

Structure Visualisation 3.1.0.0 or ORTEP-3 V2.02 for Windows XP.^{38,39} The drawn ellipsoids represent 50% probability.

3.3. Synthesis

3.3.1. Methyl 2,3,4-tri-O-benzyl- α -D-mannopyranoside (**6**)

Methyl α -D-manno-pyranoside (30.0 g, 155 mmol) and trityl chloride (90.6 g, 323 mmol) were stirred in pyridine (180 mL) at rt for 41 h under nitrogen. The brown suspension was diluted with CH_2Cl_2 (500 mL) and washed with 150 mL brine, the organic layer was separated and the aqueous layer was extracted with CH_2Cl_2 (300 mL). The organic layers were combined, dried over Na_2SO_4 , filtered, concentrated in vacuo and coevaporated with toluene to yield a brown solid residue. The crude product was diluted in dry DMF (100 mL) and this solution was slowly added to a suspension of NaH (60% in oil, 37.9 g, 926 mmol) in dry DMF (250 mL) at 0°C . After stirring for 10 min at 0°C benzyl bromide (100 mL, 924 mmol) was added slowly and the suspension was stirred 5 min at 0°C and 21 h at rt. The suspension was quenched with water (5 L), split in two fractions and each extracted with ethyl acetate ($3 \times 800 \text{ mL}$), large solvent volumes were required to separate the phases containing DMF. The organic layer was dried over Na_2SO_4 , filtered and concentrated in vacuo to obtain a brown oil. The residue was dissolved in CH_2Cl_2 (500 mL) and $\text{FeCl}_3 \cdot 6\text{H}_2\text{O}$ (194 g, 719 mmol) was added and the mixture was stirred at rt for 20 h. The reaction was quenched with saturated NaHCO_3 solution (2 L) and extracted with CH_2Cl_2 ($3 \times 3 \text{ L}$), large solvent volumes were required to separate the phases due to floating iron salts. The combined organic layers were dried over Na_2SO_4 , filtered and concentrated in vacuo to a brown oil, which was purified by silica gel chromatography (PE to PE/EtOAc 1/1). The product was obtained as orange oil (34.7 g, 48% over three steps): $R_f=0.3$ (PE/EtOAc 2/1); ^1H NMR (CDCl_3 , 400 MHz): δ 7.39–7.28 (m, 15H, Ph), 4.96 (d, $J=10.9 \text{ Hz}$, 1H, OCH_2Ph), 4.80 (d, $J=12.3 \text{ Hz}$, 1H, OCH_2Ph), 4.72–4.65 (m, 5H, H1, OCH_2Ph), 4.71 (m, 1H, OCH_2Ph), 4.67 (m, 1H, OCH_2Ph), 4.65 (s, 2H, OCH_2Ph), 3.99 (t, $J=9.4 \text{ Hz}$, 1H, H4), 3.92 (dd, $J=2.9, 9.4 \text{ Hz}$, 1H, H3), 3.86 (dd, $J=2.9, 11.6 \text{ Hz}$, 1H, H6), 3.82–3.77 (m, 2H, H2, H6), 3.64 (ddd, $J=3.0, 4.5, 9.2 \text{ Hz}$, 1H, H5), 3.32 (s, 3H, OCH_3); ^{13}C NMR (CDCl_3 , 101 MHz): δ 138.6, 138.5, 138.4, 128.5, 128.5 (3C), 128.1, 127.9, 127.8, 127.7 (2C), 99.4 (C1), 80.3 (C3), 75.3 (OCH_2Ph), 75.0 (C4), 74.8 (C2), 73.0 (OCH_2Ph), 72.3 (OCH_2Ph), 72.1 (C5), 62.5 (C6), 54.9 (OCH_3); HRMS $[\text{M}+\text{Na}]^+$: calcd 487.2091, found 487.2072.

3.3.2. Methyl 2,3,4-tri-O-benzyl- α -D-manno-hexodialdo-pyranoside (**7**)

DMSO (5.2 mL, 73.9 mmol) was added to a solution of oxalyl chloride (3.0 mL, 35.2 mmol) in dry CH_2Cl_2 (60 mL) at -75°C and stirred for 15 min. A solution of **6** (13.5 g, 29.1 mmol) in 75 mL CH_2Cl_2 was added dropwise and stirring was continued for 1 h at -75°C . Afterwards NEt_3 (10 mL, 73.9 mmol) was added and stirred for 40 min. After warming to rt the reaction mixture was quenched with saturated NH_4Cl solution (50 mL). The separated organic layer was then washed with H_2O (150 mL), the aqueous phases were extracted with CH_2Cl_2 (200 mL) and the combined organic layers were dried over Na_2SO_4 , filtered and concentrated in vacuo at 30°C . The light brown oil was purified by silica gel chromatography (PE/EtOAc 9/1 to PE/EtOAc 3/2) to give a yellow oil (10.4 g, 77%): $R_f=0.2$ (PE/EtOAc 3/1); ^1H NMR (CDCl_3 , 400 MHz): δ 9.74 (d, $J=0.7 \text{ Hz}$, 1H, CHO), 7.35–7.30 (m, 15H, Ph), 4.86–4.83 (m, 2H, H1, OCH_2Ph), 4.71–4.61 (m, 5H, OCH_2Ph), 4.10–4.03 (m, 2H, H4, H5), 3.95 (dd, $J=2.9, 7.9 \text{ Hz}$, 1H, H3), 3.77 (t, $J=2.8 \text{ Hz}$, 1H, H2), 3.38 (s, 3H, OCH_3); ^{13}C NMR (CDCl_3 , 101 MHz): δ 198.0 (CHO), 138.2 (2C), 137.9, 128.5, 128.5, 128.5, 128.4, 128.0, 128.0, 127.9, 127.8, 127.8, 99.6 (C1), 79.3 (C3), 76.2 (C4), 74.8 (OCH_2Ph), 74.5 (C5), 74.3 (C2), 73.0

(OCH₂Ph), 72.4 (OCH₂Ph), 55.6 (OCH₃); HRMS [M+Na]⁺: calcd 485.1935, found 485.1916.

3.3.3. Methyl 2,3-di-O-benzyl-4-deoxy-6-aldehydo-β-L-erythro-hex-4-enodialdo-1,5-pyranoside (**8**)

The reaction was performed as described for **7** with the following amounts: oxalyl chloride (0.7 mL, 8.2 mmol), DMSO (1.1 mL, 16 mmol), NEt₃ (4.4 mL, 32 mmol) and **6** (1.84 mg, 4.0 mmol) in CH₂Cl₂ (20 mL). The workup was performed as follows: The reaction mixture was washed with H₂O (40 mL) and the aqueous layer was extracted with CH₂Cl₂ (40 mL). The combined organic phases were dried over Na₂SO₄, filtered and concentrated in vacuo at 40 °C. After the purification by silica gel chromatography (PE/EtOAc 9/1 to 1/1), **7** (0.63 g, 34%) and a yellowish oil of **8** was obtained (0.47 g, 33%); R_f=0.3 (PE/EtOAc 3/1); IR (ATR): 2933 (w), 2863 (w), 1698 (s), 1640 (m), 1496 (m), 1454 (m), 1347 (m), 1313 (m), 1200 (m), 1180 (m), 1143 (s), 1121 (s), 1074 (s), 1026 (s), 959 (s), 894 (s), 817 (m), 736 (s); ¹H NMR (CDCl₃, 400 MHz): δ 9.18 (s, 1H, CHO), 7.38–7.30 (m, 10H, Ph), 5.93 (dd, J=1.6, 2.5 Hz, 1H, H4), 5.10 (d, J=2.9 Hz, 1H, H1), 4.74 (s, 2H, OCH₂Ph), 4.63 (d, J=1.9 Hz, 2H, OCH₂Ph), 4.42 (dd, J=2.5, 4.1 Hz, 1H, H3), 3.83 (ddd, J=1.6, 3.0, 4.4 Hz, 1H, H2), 3.46 (s, 3H, CH₃); ¹³C NMR (CDCl₃, 101 MHz): δ 186.3 (CHO), 148.8 (C5), 137.8, 128.6, 128.6, 128.5, 128.1, 128.1, 128.0, 127.7, 121.1 (C4), 99.9 (C1), 73.0 (OCH₂Ph), 71.6 (OCH₂Ph), 70.4 (C2), 70.2 (C3), 56.7 (CH₃); HRMS [M+Na]⁺: calcd 377.1359, found 377.1337.

3.3.4. Methyl 2,3,4-tri-O-benzyl-(6S)-cyano-α-D-mannopyranoside (**9a**), methyl 2,3,4-tri-O-benzyl-(6R)-cyano-α-D-mannopyranoside (**9b**)

KCN (113 mg, 1.74 mmol) was dissolved in 0.15 mL saturated aqueous NH₄Cl solution and cooled to 0 °C. **7** (96.0 mg, 0.20 mmol) in MeOH (0.4 mL) was added dropwise and stirred for 5 min at 0 °C and 1 h at rt. The reaction mixture was adjusted to pH=8 and extracted with 30 mL EtOAc. The organic phase was dried over Na₂SO₄, filtered and concentrated in vacuo at 30 °C. The crude product was purified by silica gel chromatography (PE/EtOAc 4/1) to give a colorless crystalline solid **9a** (49.0 mg, 50%) and a colorless oil **9b** (22.0 mg, 22%). **9a**: [α]_D²⁴+23.4 (c 0.61, CHCl₃); R_f=0.5 (PE/EtOAc 3/1); ¹H NMR (CDCl₃, 400 MHz): δ 7.42–7.26 (m, 15H), 5.00 (d, J=11.0 Hz, 1H, OCH₂Ph), 4.80 (d, J=1.7 Hz, 1H, H-1), 4.78 (d, J=12.4 Hz, 1H, OCH₂Ph), 4.68 (d, J=12.5 Hz, 1H, OCH₂Ph), 4.68 (d, J=1.1 Hz, 1H, H-6), 4.65 (d, J=11.9 Hz, 1H, OCH₂Ph), 4.63 (s, 2H, OCH₂Ph), 4.11 (t, J=9.6 Hz, 1H, H-4), 3.93 (dd, J=9.5, 3.0 Hz, 1H, H-3), 3.83 (dd, J=2.9, 1.8 Hz, 1H, H-2), 3.74 (dd, J=9.7, 1.1 Hz, 1H, H-5); ¹³C NMR (CDCl₃, 101 MHz): δ 138.1, 138.0, 137.9, 128.6, 128.6, 128.5, 128.1, 128.1, 128.0, 127.9, 127.8, 127.7, 118.5 (CN), 99.8 (C1), 80.0 (C3), 75.5 (OCH₂Ph), 74.6 (C2), 73.4 (C4), 73.2 (OCH₂Ph), 72.3 (C5), 72.3 (OCH₂Ph), 61.1 (C6), 55.3 (OCH₃); HRMS [M+Na]⁺: calcd 512.2044, found 512.2047. **9b**: [α]_D²⁴+42.2 (c 0.54, CHCl₃); R_f=0.3 (PE/EtOAc 3/1); ¹H NMR (CDCl₃, 400 MHz): δ 7.39–7.27 (m, 15H, Ph), 5.01 (d, J=11.0 Hz, 1H, OCH₂Ph), 4.80–4.75 (m, 2H, H-1, OCH₂Ph), 4.72 (d, J=4.0 Hz, 1H, H-6), 4.68 (d, J=12.4 Hz, 1H, OCH₂Ph), 4.67 (d, J=11.0 Hz, 1H, OCH₂Ph), 4.63 (d, J=11.7 Hz, 1H, OCH₂Ph), 4.60 (d, J=11.7 Hz, 1H, OCH₂Ph), 4.09 (t, J=9.5 Hz, 1H, H-4), 3.93 (dd, J=9.2, 3.0 Hz, 1H, H-3), 3.82–3.81 (m, 1H, H-2), 3.80 (dd, J=10.0, 4.0 Hz, 1H, H-5), 3.33 (s, 3H, OCH₃); ¹³C NMR (CDCl₃, 101 MHz): δ 138.1, 138.1, 137.7, 128.7, 128.6, 128.5, 128.2, 128.2, 127.9, 127.8, 127.8 (2C), 117.3 (CN), 99.5 (C1), 80.0 (C3), 75.5 (OCH₂Ph), 75.5 (C4), 74.4 (C2), 72.9 (OCH₂Ph), 72.1 (OCH₂Ph), 71.8 (C5), 63.0 (C6), 55.4 (OCH₃); HRMS [M+Na]⁺: calcd 512.2044, found 512.2011.

3.3.5. General procedure for synthesis of methyl 2,3,4-tri-O-benzyl-α-D-manno-7-amino-7-deoxy-heptapyranoside (**10a**, **10b**)

LiAlH₄ (4.5 equiv) was suspended in dry THF (1 mL/mmol hydride LiAlH₄) and cooled to 0 °C. A solution of cyanohydrin (1 equiv)

in dry THF (2 mL/mmol nitrile) was added dropwise and stirred for 5 min at 0 °C and further 10 min at rt. The reaction was first quenched with 0.1 mL of 0.1 M NaOH solution per 1 mmol LiAlH₄ and extracted with EtOAc. The separated organic phase was dried over Na₂SO₄, filtered and concentrated in vacuo. The crude product was purified by silica gel chromatography (CH₂Cl₂/EtOAc/MeOH 1/0 to CH₂Cl₂/EtOAc/MeOH 1/1/1).

3.3.5.1. Methyl 2,3,4-tri-O-benzyl-(6S)-α-D-manno-7-amino-7-deoxy-heptapyranoside (10a**)**. LiAlH₄ (2.00 g, 52.7 mmol) in 50 mL THF and **9a** (5.80 g, 11.8 mmol) in 100 mL THF yielded 4.87 g (84%) of a yellowish oil: [α]_D²⁴+21.2 (c 0.87, CHCl₃); R_f=0.4 (CH₂Cl₂/MeOH/EtOAc 2/1/1); ¹H NMR (CDCl₃, 400 MHz): δ 7.38–7.24 (m, 15H, Ph), 4.97 (d, J=10.8 Hz, 1H, OCH₂Ph), 4.80–4.68 (m, 4H, H1, OCH₂Ph), 4.64 (s, 2H, OCH₂Ph), 4.15 (t, J=9.5 Hz, 1H, H4), 3.88 (dd, J=3.0, 9.3 Hz, 1H, H3), 3.84 (ddd, J=1.2, 4.1, 7.8 Hz, 1H, H6), 3.79 (dd, J=1.9, 2.9 Hz, 1H, H2), 3.50 (d, J=9.6 Hz, 1H, H5), 3.28 (s, 3H, OCH₃), 2.93 (dd, J=8.0, 12.9 Hz, 1H, H7), 2.76 (dd, J=4.2, 12.9 Hz, 1H, H7); ¹³C NMR (CDCl₃, 101 MHz): δ 138.7, 138.6, 138.4, 128.5 (3C), 128.0, 127.9, 127.8, 127.7, 127.7, 127.6, 99.6 (C1), 80.3 (C3), 75.3 (OCH₂Ph), 74.7 (2C, C2, C4), 73.0 (OCH₂Ph), 72.7 (C5), 72.3 (OCH₂Ph), 70.3 (C6), 54.8 (OCH₃), 45.3 (C7); HRMS [M+H]⁺: calcd 494.2537, found 494.2516.

3.3.5.2. Methyl 2,3,4-tri-O-benzyl-(6R)-α-D-manno-7-amino-7-deoxy-heptapyranoside (10b**)**. LiAlH₄ (432 mg, 11.4 mmol) in 10 mL THF and **9b** (1.30 g, 2.65 mmol) in 20 mL THF yielded 777 mg (60%) of a yellowish oil: [α]_D²⁴+41.7 (c 0.38, CHCl₃); R_f=0.4 (CH₂Cl₂/MeOH/EtOAc 2/1/1); ¹H NMR (CDCl₃, 400 MHz): δ 7.36–7.27 (15H, Ph), 4.99 (d, J=11.0 Hz, 1H, OCH₂Ph), 4.77–4.56 (m, 5H, H1, OCH₂Ph), 3.98–3.90 (m, 2H, H3, H4), 3.82 (dd, J=5.2, 10.2 Hz, 1H, H6), 3.78 (m, 1H, H2), 3.66 (dd, J=4.7, 8.7 Hz, 1H, H5), 3.32 (s, 3H, OCH₃), 2.83 (d, J=5.3 Hz, 2H, H7); ¹³C NMR (CDCl₃, 101 MHz): δ 138.3, 138.3, 138.1, 128.6, 128.5, 128.5, 128.3, 128.2, 128.0, 127.8, 127.8 (2C), 99.1 (C1), 80.6 (C3), 76.5 (C4), 74.9 (OCH₂Ph), 74.7 (C2), 72.9 (OCH₂Ph), 72.8 (C6), 72.3 (C5), 72.1 (OCH₂Ph), 55.0 (OCH₃), 43.2 (C7); HRMS [M+H]⁺: calcd 494.2537, found 494.2518.

3.3.6. General procedure of debenzylation

To a mixture of methyl 2,3,4-tri-O-benzyl-α-D-manno-7-amino-7-deoxy-heptapyranoside in H₂O and THF, TFA and Pd/C 10% were added. The reaction mixture was stirred under H₂ atmosphere at rt and atmospheric pressure. After TLC indicated completion of the reaction, it was filtered through a Celite pad and concentrated in vacuo to yield a colorless solid, which was used as starting material for the next steps without further purification.

3.3.6.1. Methyl (6S)-α-D-manno-7-amino-7-deoxy-heptapyranoside (11a**)**. **10a** (4.49 g, 9.09 mmol) in a mixture of H₂O (200 mL) and THF (800 mL), TFA (3.5 mL) and 10% (w/w) Pd/C (451 mg) yielded after 3 d stirring under H₂ atmosphere a colorless solid: R_f=0.05 (CH₂Cl₂/MeOH/NEt₃/H₂O 8/3/0.5/0.5); ¹H NMR (MeOH-d₄, 400 MHz): δ 4.69 (d, J=1.7 Hz, 1H, H1), 4.14 (ddd, J=2.1, 3.4, 9.4 Hz, 1H, H6), 3.83 (t, J=9.6 Hz, 1H, H4), 3.80 (dd, J=1.9, 3.5 Hz, 1H, H2), 3.67 (dd, J=3.3, 9.5 Hz, 1H, H3), 3.43 (dd, J=2.2, 9.7 Hz, 1H, H5), 3.36 (s, 3H, OCH₃), 3.16 (dd, J=9.4, 12.7 Hz, 1H, H7), 3.09 (dd, J=3.5, 12.8 Hz, 1H, H7); ¹³C NMR (MeOH-d₄, 101 MHz): δ 103.1 (C1), 74.2 (C5), 72.4 (C3), 71.8 (C2), 67.7 (C4), 67.2 (C6), 55.5 (OCH₃), 44.1 (C7); HRMS [M+H]⁺: calcd 224.1129, found 224.1125.

3.3.6.2. Methyl (6R)-α-D-manno-7-amino-7-deoxy-heptapyranoside (11b**)**. **10b** (777 mg, 1.57 mmol) in a mixture of H₂O (45 mL) and THF (120 mL), TFA (500 μL) and 10% (w/w) Pd/C (80.0 mg) yielded after 2 d stirring under H₂ atmosphere a colorless solid: R_f=0.1 (CH₂Cl₂/MeOH/NEt₃/H₂O 8/3/0.5/0.5); ¹H NMR (MeOH-d₄,

400 MHz): δ 4.66 (d, $J=1.6$ Hz, 1H, H1), 4.17 (ddd, $J=1.7, 4.0, 6.2$ Hz, 1H, H6), 3.80 (dd, $J=1.7, 2.9$ Hz, 1H, H2), 3.67–3.61 (m, 3H, H3, H4, H5), 3.39 (s, 3H, OCH₃), 3.20 (dd, $J=6.7, 13.1$ Hz, 1H, H7), 3.14 (dd, $J=4.1, 13.1$ Hz, 1H, H7); ¹³C NMR (MeOH-*d*₄, 101 MHz): δ 102.8 (C1), 75.7 (C5), 72.5 (C3), 71.8 (C2), 69.0 (C4), 68.1 (C6), 55.4 (OCH₃), 41.9 (C7); HRMS [M+H]⁺: calcd 224.1129, found 224.1126.

3.3.7. Methyl (6S)- α -D-manno-7-(benzamido)-7-deoxyheptapyranoside (**4a**)

Crude **11a** (50 mg) was dissolved in 2 mL DMF, NEt₃ (78 μ L, 0.56 mmol) was added and the mixture was cooled to 0 °C. After dropwise addition of benzoyl chloride (31 μ L, 0.27 mmol) the reaction mixture was stirred for 1 h at 0 °C and was then allowed to warm to rt. The mixture was diluted with EtOAc (10 mL) and washed with saturated NH₄Cl solution (30 mL). The organic phase was dried over Na₂SO₄, filtered and concentrated in vacuo. Incubation of the crude product with acidic ion exchange resin Amberlite IR-120 in 2 mL MeOH to remove excess NEt₃ and purification by silica gel chromatography (EtOAc to EtOAc/EtOH/NH₄OH aq (25%) ratio 5/5/1) yielded 25.6 mg of a colorless solid (0.08 mmol, 71% over two steps): $R_f=0.2$ (CH₂Cl₂/EtOH 4/1); ¹H NMR (MeOH-*d*₄, 400 MHz): δ 7.85–7.83 (m, 2H, Ph), 7.55–7.51 (m, 1H, Ph), 7.48–7.44 (m, 2H, Ph), 4.70 (s, 1H, H1), 4.20 (dd, $J=4.9, 7.2$ Hz, 1H, H6), 3.87 (t, $J=9.6$ Hz, 1H, H4), 3.79 (dd, $J=1.5, 3.0$ Hz, 1H, H2), 3.73–3.67 (m, 2H, H3, H7), 3.56–3.49 (m, 2H, H5, H7), 3.38 (s, 3H, OCH₃); ¹³C NMR (MeOH-*d*₄, 101 MHz): δ 170.5, 135.7, 132.6, 129.5 (2C), 128.2 (2C), 103.1 (C1), 73.9 (C5), 72.6 (C3), 72.1 (C2), 68.8 (C6), 67.9 (C4), 55.5 (OCH₃), 44.9 (C7); HRMS [M+Na]⁺: calcd 350.1210, found 350.1203.

3.3.8. Methyl (6S)- α -D-manno-7-(cinnamido)-7-deoxyheptapyranoside (**4b**)

A mixture of **11a** (70.0 mg) and NEt₃ (44 μ L, 0.32 mmol) in DMF (1.5 mL) was cooled to 0 °C. After the slow addition of cinnamoyl chloride (33.3 mg, 0.20 mmol) in 0.5 mL DMF the reaction mixture was stirred further 30 min at 0 °C and 24 h at rt. After removal of the solvent in vacuo the crude product was directly purified by HPLC to obtain 18.3 mg (0.05 mmol, 34% over two steps) of a colorless solid: R_f (CH₂Cl₂/EtOH 8/1) 0.1; ¹H NMR (MeOH-*d*₄, 600 MHz): δ 7.57–7.53 (m, 3H), 7.41–7.36 (m, 3H), 6.67 (d, $J=15.8$ Hz, 1H), 4.69 (s, 1H, H1), 4.12–4.09 (m, 1H, H6), 3.84 (t, $J=3.8$ Hz, 1H, H4), 3.78 (dd, $J=1.7, 3.4$ Hz, 1H, H2), 3.67 (dd, $J=3.4, 9.6$ Hz, 1H, H3), 3.63 (dd, $J=4.8, 13.5$ Hz, 1H, H7), 3.48–3.42 (m, 2H, H5, H7), 3.38 (s, 3H, OCH₃); ¹³C NMR (MeOH-*d*₄, 151 MHz): δ 168.9, 141.7, 136.3, 130.8, 129.9 (2C), 128.8 (2C), 121.9, 103.0 (C1), 73.8 (C5), 72.7 (C3), 72.1 (C2), 68.9 (C6), 67.9 (C4), 55.5 (CH₃), 44.4 (C7); HRMS [M+Na]⁺: calcd 376.1367, found 376.1340.

3.3.9. Methyl (6S)- α -D-manno-7-(acetamido)-7-deoxyheptapyranoside (**4c**)

To a mixture of crude **11a** (70 mg) in DMF (1.5 mL) NEt₃ (44 μ L, 0.32 mmol) was added dropwise and the reaction was cooled to 0 °C. After slow addition of acetic anhydride (20 μ L, 0.21 mmol) in DMF (0.5 mL), the reaction mixture continued stirring for further 45 min at 0 °C and 24 h at rt. Afterwards the mixture was quenched with saturated NaHCO₃ solution and was allowed to stir further 30 min. After concentration in vacuo the crude product was directly purified by preparative HPLC to obtain colorless solid (27.4 mg, 67% over two steps): $R_f=0.4$ (CH₂Cl₂/EtOH 2/1); ¹H NMR (MeOH-*d*₄, 500 MHz): δ 4.67 (d, $J=1.7$ Hz, 1H, H1), 4.02 (ddd, $J=8.6, 4.7, 1.6$ Hz, 1H, H-6), 3.82 (t, $J=9.7$ Hz, 1H, H-4), 3.77 (dd, $J=3.4, 1.7$ Hz, 1H, H-2), 3.66 (dd, $J=9.6, 3.4$ Hz, 1H, H-3), 3.47 (dd, $J=13.6, 4.7$ Hz, 1H, H-7), 3.41 (dd, $J=9.8, 1.6$ Hz, 1H, H-5), 3.36 (s, 3H, OCH₃), 3.34–3.25 (m,

1H, H-7), 1.97 (s, 3H, Ac). ¹³C NMR (MeOH-*d*₄, 101 MHz): δ 173.6, 103.0 (C1), 73.7 (C5), 72.6 (C3), 72.0 (C2), 68.7 (C6), 67.8 (C4), 55.5 (OCH₃), 44.3 (C7), 22.6 (CH₃); HRMS [M+Na]⁺: calcd 288.1054, found 288.1048.

3.3.10. Methyl (6S)- α -D-manno-7-(2-mesitylenesulfonamido)-7-deoxyheptapyranoside (**4d**)

To crude **11a** (70.0 mg) in DMF (1.5 mL), NEt₃ (44 μ L, 0.32 mmol) was added and the mixture was cooled to 0 °C. Afterwards the 2-mesitylenesulfonyl chloride (45.3 mg, 0.21 mmol) in DMF (0.5 mL), was added dropwise and the reaction mixture stirred 30 min under cooling and 26 h at rt. After removal of the solvent the crude product was directly purified by HPLC to obtain 20.1 mg (0.05 mmol, 32% over two steps): $R_f=0.6$ (EtOAc/EtOH/NH₄OH(25%) 2/2/1); ¹H NMR (MeOH-*d*₄, 500 MHz): δ 7.02 (s, 2H, Ph), 4.61 (d, $J=1.5$ Hz, 1H, H1), 3.95 (ddd, $J=1.8, 5.3, 7.4$ Hz, 1H, H6), 3.78–3.73 (m, 2H, H2, H4), 3.63 (dd, $J=3.4, 9.5$ Hz, 1H, H3), 3.39 (dd, $J=1.7, 9.8$ Hz, 1H, H5), 3.30 (s, 3H, OCH₃), 3.07 (dd, $J=5.2, 12.7$ Hz, 1H, H7), 2.96 (dd, $J=7.8, 12.7$ Hz, 1H, H7), 2.62 (s, 6H, PhCH₃), 2.30 (s, 3H, PhCH₃); ¹³C NMR (MeOH-*d*₄, 101 MHz): δ 143.5, 140.3 (2C), 135.1, 132.9 (2C), 102.9 (C1), 73.4 (C5), 72.6 (C3), 72.01 (C2), 68.8 (C6), 67.8 (C4), 55.5 (OCH₃), 46.7 (C7), 23.1 (2C, CH₃), 20.9 (CH₃); LCMS [M+H]⁺: calcd 406.2, found 405.9.

3.3.11. Methyl (6S)- α -D-manno-7-(*p*-toluylsulfonamido)-7-deoxyheptapyranoside (**4e**)

To crude **11a** (70.0 mg) in DMF (1.5 mL), NEt₃ (44 μ L, 0.32 mmol) was added and the mixture was cooled to 0 °C. Afterwards tosyl chloride (39.8 mg, 0.21 mmol) in DMF (0.5 mL) was added dropwise and the reaction mixture stirred 30 min under cooling and 26 h at rt. After removal of the solvent the crude product was directly purified by HPLC to obtain 31.6 mg (0.08 mmol, 54% over two steps): $R_f=0.6$ (EtOAc/EtOH/NH₄OH(25%) 2/2/1); ¹H NMR (MeOH-*d*₄, 400 MHz): δ 7.74 (d, $J=8.4$ Hz, 2H, Ph), 7.38 (d, $J=8.2$ Hz, 2H, Ph), 4.63 (d, $J=1.8$ Hz, 1H, H1), 3.98 (ddd, $J=7.5, 6.2, 1.7$ Hz, 1H, H6), 3.79 (dd, $J=9.7, 9.7$ Hz, 1H, H4), 3.76–3.74 (m, 1H, H2), 3.65 (dd, $J=9.6, 3.2$ Hz, 1H, H3), 3.47 (dd, $J=9.8, 1.7$ Hz, 1H, H5), 3.33 (s, 3H, OCH₃), 3.10 (dd, $J=12.5, 6.2$ Hz, 1H, H7), 2.90 (dd, $J=12.5, 7.4$ Hz, 1H, H7), 2.42 (s, 3H, PhCH₃); ¹³C NMR (MeOH-*d*₄, 101 MHz): δ 144.6, 138.5, 130.7 (2C), 128.1 (2C), 102.9 (C1), 73.0 (C5), 72.6 (C3), 72.0 (C2), 68.9 (C6), 67.7 (C4), 55.6 (OCH₃), 47.1 (C7), 21.4 (PhCH₃), LCMS [M+Na]⁺: calcd 400.1, found 399.8.

3.3.12. Methyl (6R)- α -D-manno-7-(benzamido)-7-deoxyheptapyranoside (**5a**)

To a solution of crude **11b** (49.0 mg) in 7 mL DMF, NEt₃ (89.0 μ L, 0.64 mmol) was added and the mixture was cooled to 0 °C. Benzoyl chloride (31.1 μ L, 0.27 mmol) was added dropwise and stirred for 30 min at 0 °C and further 30 min at rt. After removing the solvent in vacuo the product was directly purified by silica gel chromatography (CH₂Cl₂/EtOH 95/5 to 8/1). Incubation of the product with acidic ion exchange resin Amberlite IR-120 in 5 mL MeOH to remove excess NEt₃ for 1 h at rt, filtration, concentration in vacuo and subsequent purification by HPLC gave the title compound as a colorless solid (16.0 mg, 0.05 mmol, 17% over two steps): $R_f=0.5$ (CH₂Cl₂/EtOH 4/1); ¹H NMR (MeOH-*d*₄, 400 MHz): δ 7.86–7.83 (m, 2H, Ph), 7.53–7.51 (m, 1H, Ph), 7.48–7.44 (m, 2H, Ph), 4.66 (d, $J=1.5$ Hz, 1H, H1), 4.13 (dt, $J=3.8, 7.5$ Hz, 1H, H6), 3.82–3.76 (m, 3H, H2, H4, H7), 3.67 (dd, $J=3.3, 9.3$ Hz, 1H, H3), 3.62–3.55 (m, 2H, H5, H7), 3.38 (s, 3H, OCH₃); ¹³C NMR (MeOH-*d*₄, 101 MHz): δ 170.6, 135.7, 132.6, 129.5, 128.3, 102.8 (C1), 74.9 (C5), 72.7 (C3), 71.8 (C2), 71.7 (C6), 69.7 (C4), 55.3 (OCH₃), 43.3 (C7); HRMS [M+Na]⁺: calcd 350.1210, found 350.1196.

3.3.13. Methyl (6R)- α -D-manno-7-(cinnamido)-7-deoxy-heptapyranoside (**5b**)

To a mixture of **11b** (49.0 mg) in DMF (7 mL) NEt₃ (87 μ L, 0.63 mmol) and EDC⁺HCl (66.0 mg, 0.34 mmol) were added. After cooling to 0 °C, cinnamic acid (44.0 mg, 0.29 mmol) was added portion wise and the reaction mixture was allowed to warm to rt and stirring was continued for 20 h. After removal of the volatiles and purification by silica gel chromatography (CH₂Cl₂/EtOH 19/1) the product was dissolved in MeOH (4 mL) and incubated with acidic ion exchange resin Amberlite IR-120 to remove excess NEt₃ for 1 h at rt. Filtration, concentration in vacuo and subsequent purification by HPLC gave the title compound as a colorless solid (10.0 mg, 0.03 mmol, 10% over two steps) was isolated: *R*_f (CH₂Cl₂/EtOH 8/1) 0.2; ¹H NMR (MeOH-*d*₄, 400 MHz): δ 7.58–7.53 (m, 3H), 7.41–7.36 (m, 3H), 6.69 (d, *J*=15.8 Hz, 1H), 4.65 (d, *J*=1.2 Hz, 1H, H1), 4.05 (dt, *J*=3.7, 7.6 Hz, 1H, H6), 3.79–3.65 (m, 4H, H2, H3, H4, H7), 3.56 (dd, *J*=3.9, 9.7 Hz, 1H, H5), 3.50 (dd, *J*=7.9, 13.9 Hz, 1H, H7), 3.38 (s, 3H, OCH₃); ¹³C NMR (MeOH-*d*₄, 151 MHz): δ 169.0, 141.7, 136.3, 130.8, 129.9, 128.8, 121.9, 102.8 (C1), 74.5 (C5), 72.6 (C3), 72.0 (C6), 71.8 (C2), 70.0 (C4), 55.3 (CH₃), 42.8 (C7); HRMS [M+Na]⁺: calcd 376.1367, found 376.1343.

3.4. Evaluation of compounds for LecB inhibition

All final compounds described in this study were evaluated in a competitive binding experiment for inhibition of LecB. The assay is run in black 384-well plates (Greiner BioOne, Germany) and is based on the displacement of a LecB-bound FITC-labelled tracer (fluorescein-fucose conjugate, details see Hauck et al.²¹) and fluorescence polarization readout in a microplate reader (Pherastar FS, BMGlabtech, Germany; ex. 485 nm, em. 525 nm) as previously described.²¹

Acknowledgments

The authors are grateful to Philipp Voss for initial experiments, Holger Bußkamp for HR-MS measurements and Dr. Josef Zapp and Anke Friemel for excellent support in NMR analyses. Dr. Anne Imberty is acknowledged for sharing the expression plasmid of LecB. We thank the Helmholtz Association [VH-NG-934], the Konstanz Research School Chemical Biology, the Zukunftskolleg, and the Deutsche Forschungsgemeinschaft [Ti756/2-1] for financial support.

Supplementary data

Supplementary data (¹H NMR and ¹³C NMR traces of all synthesized compounds, temperature dependent ¹H NMR spectra and data of J-HMBC measurements for **9a** and **9b**) related to this article can be found at <http://dx.doi.org/10.1016/j.carres.2015.04.010>.

References

1. Yahr T, Parsek M. *The prokaryotes volume 6: Proteobacteria: gamma subclass*. 3 ed., vol. 6. Springer-Verlag; 2006.
2. Peleg AY, Hooper DC. *New Engl J Med* 2010; **362**: 1804–13.
3. Tümmler B, Kiewitz C. *Mol Med Today* 1999; **5**: 351–8.
4. Davies D. *Nat Rev Drug Discov* 2003; **2**: 114–22.
5. Poole K. *Front Microbiol* 2011; **2**: 65.
6. Flemming H-C, Wingender J. *Nat Rev Microbiol* 2010; **8**: 623–33.
7. Tielker D, Hacker S, Loris R, Strathmann M, Wingender J, Wilhelm S, et al. *Microbiology* 2005; **151**: 1313–23.
8. Diggle SP, Stacey RE, Dodd C, Cámara M, Williams P, Winzer K. *Environ Microbiol* 2006; **8**: 1095–104.
9. Gilboa-Garber N, Mizrahi L, Garber N. *Can J Biochem* 1977; **55**: 975–81.
10. Gilboa-Garber N. *Methods Enzymol* 1982; **83**: 378–85.
11. Mitchell E, Houles C, Sudakevitz D, Wimmerova M, Gautier C, Pérez S, et al. *Nat Struct Biol* 2002; **9**: 918–21.
12. Loris R, Tielker D, Jaeger K-E, Wyns L. *J Mol Biol* 2003; **331**: 861–70.
13. Sabin C, Mitchell EP, Pokorná M, Gautier C, Utille J-P, Wimmerová M, et al. *FEBS Lett* 2006; **580**: 982–7.
14. Perret S, Sabin C, Dumon C, Pokorná M, Gautier C, Galanina O, et al. *Biochem J* 2005; **389**: 325–26.
15. Imberty A, Chabre YM, Roy R. *Chem Eur J* 2008; **14**: 7490–9.
16. Bernardi A, Jiménez-Barbero J, Casnati A, De Castro C, Darbre T, Fieschi F, et al. *Chem Soc Rev* 2012; **42**: 4709–27.
17. Sommer R, Joachim I, Wagner S, Titz A. *CHIMIA* 2013; **67**: 286–90.
18. Titz A. In: Seeberger PH, Rademacher C, editors. *Carbohydrates as drugs topics in medicinal chemistry*. Springer Berlin Heidelberg; 2014. p. 169–86.
19. Johansson EMV, Cruz SA, Kolomiets E, Buts L, Kadam RU, Cacciarini M, et al. *Chem Biol* 2008; **15**: 1249–57.
20. Boukerb AM, Rousset A, Galanos N, Méar J-B, Thepaut M, Grandjean T, et al. *J Med Chem* 2014; **57**: 10275–89.
21. Hauck D, Joachim I, Frommeyer B, Varrot A, Philipp B, Möller HM, et al. *ACS Chem Biol* 2013; **8**: 1775–84.
22. Sommer R, Exner TE, Titz A. *PLoS One* 2014; **9**: e112822.
23. Titz A, Marra A, Cutting B, Smiesko M, Papandreou G, Dondoni A, et al. *Eur J Org Chem* 2012; 5534–9.
24. Titz A, Patton J, Alker AM, Porro M, Schwardt O, Hennig M, et al. *Bioorg Med Chem* 2008; **16**: 1046–56.
25. Titz A, Ernst B. *CHIMIA* 2007; **61**: 194–7.
26. Schwizer D, Patton JT, Cutting B, Smiesko M, Wagner B, Kato A, et al. *Chem Eur J* 2012; **18**: 1342–51.
27. Binder FPC, Lemme K, Preston RC, Ernst B. *Angew Chem Int Ed Engl* 2012; **51**: 7327–31.
28. Boren HB, Eklind K, Garegg PJ, Lindberg B, Pilotti A. *Acta Chem. Scand* 1972; **26**: 4143–6.
29. Ding X, Wang W, Kong F. *Carbohydr Res* 1997; **303**: 445–8.
30. Mackie DM, Perlin AS. *Carbohydr Res* 1972; **24**: 67–85.
31. Meissner A, Sørensen OW. *Magn Res Chem* 2001; **39**: 49–52.
32. Lu Y, Miet C, Kunesch N, Poisson JE. *Tetrahedron: Asymmetry* 1993; **4**: 893–902.
33. Dziewiszek K, Zamojski A. *Carbohydr Res* 1986; **150**: 163–71.
34. Deunf E, Zaborova E, Guieu S, Blériot Y, Verpeaux J-N, Buriez O, et al. *Eur J Inorg Chem* 2010; 4720–7.
35. Rylander. *Hydrogenation methods*. Academic Press; 1985.
36. X-RED version 1.31. *Stoe data reduction program*. Darmstadt, Germany. 2005.
37. Sheldrick GM. *SHELXS-97 program for crystal structure analysis*. Germany: University of Göttingen; 1997.
38. Faruggia IJ. *ORTEP-3 V2.02 for windows XP*. Scotland: University of Glasgow; 2008.
39. *Diamond—crystal and molecular structure visualization, crystal impact*. Dr. H. Putz & Dr. K. Brandenburg, GbR: Bonn, Germany.